



The combined effects of acidification and hypoxia on pH and aragonite saturation in the coastal waters of the California current ecosystem and the northern Gulf of Mexico



Richard A. Feely^{a,*}, Remy R. Okazaki^b, Wei-Jun Cai^c, Nina Bednaršek^d, Simone R. Alin^a, Robert H. Byrne^e, Andrea Fassbender^f

^a Pacific Marine Environmental Laboratory/NOAA, 7600 Sand Point Way NE, Seattle, WA 98115, USA

^b Joint Institute for the Study of the Atmosphere and Oceans, University of Washington, Box 355672, Seattle, WA 98195-5672, USA

^c School of Marine Science and Policy, University of Delaware, College of Earth, Ocean, and Environment, 111 Robinson Hall, Newark, DE 19716, USA

^d Southern California Coastal Water Research Project Authority, 3535 Harbor Blvd., Suite 110, Costa Mesa, CA 92626, USA

^e College of Marine Science, University of South Florida, 140 7th Ave S, St. Petersburg, FL 33701, USA

^f Monterey Bay Aquarium Research Institute, 7700 Sandholt Road, Moss Landing, CA 95039, USA

ARTICLE INFO

Keywords:

Ocean acidification
CaCO₃ undersaturation
Hypercapnia
Hypoxia

ABSTRACT

Inorganic carbon chemistry data from the surface and subsurface waters of the West Coast of North America have been compared with similar data from the northern Gulf of Mexico to demonstrate how future changes in CO₂ emissions will affect chemical changes in coastal waters affected by respiration-induced hypoxia ([O₂] ≤ ~ 60 μmol kg⁻¹). In surface waters, the percentage change in the carbon parameters due to increasing CO₂ emissions are very similar for both regions even though the absolute decrease in aragonite saturation is much higher in the warmer waters of the Gulf of Mexico. However, in subsurface waters the changes are enhanced due to differences in the initial oxygen concentration and the changes in the buffer capacity (i.e., increasing Revelle Factor) with increasing respiration from the oxidation of organic matter, with the largest impacts on pH and CO₂ partial pressure (pCO₂) occurring in the colder West Coast waters. As anthropogenic CO₂ concentrations begin to build up in subsurface waters, increased atmospheric CO₂ will expose organisms to hypercapnic conditions (pCO₂ > 1000 μatm) within subsurface depths. Since the maintenance of the extracellular pH appears as the first line of defense against external stresses, many biological response studies have been focused on pCO₂-induced hypercapnia. The extent of subsurface exposure will occur sooner and be more widespread in colder waters due to their capacity to hold more dissolved oxygen and the accompanying weaker acid-base buffer capacity. Under present conditions, organisms in the West Coast are exposed to hypercapnic conditions when oxygen concentrations are near 100 μmol kg⁻¹ but will experience hypercapnia at oxygen concentrations of 260 μmol kg⁻¹ by year 2100 under the highest elevated-CO₂ conditions. Hypercapnia does not occur at present in the Gulf of Mexico but will occur at oxygen concentrations of 170 μmol kg⁻¹ by the end of the century under similar conditions. The aragonite saturation horizon is currently above the hypoxic zone in the West Coast. With increasing atmospheric CO₂, it is expected to shoal up close to surface waters under the IPCC Representative Concentration Pathway (RCP) 8.5 in West Coast waters, while aragonite saturation state will exhibit steeper gradients in the Gulf of Mexico. This study demonstrates how different biological thresholds (e.g., hypoxia, CaCO₃ undersaturation, hypercapnia) will vary asymmetrically because of local initial conditions that are affected differently with increasing atmospheric CO₂. The direction of change in amplitude of hypercapnia will be similar in both ecosystems, exposing both biological communities from the West Coast and Gulf of Mexico to intensification of stressful conditions. However, the region of lower Revelle factors (i.e., the Gulf of Mexico), currently provides an adequate refuge habitat that might no longer be the case under the most severe RCP scenarios.

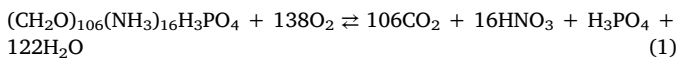
* Corresponding author.

E-mail address: richard.a.feely@noaa.gov (R.A. Feely).

1. Introduction

The decrease in pH and aragonite saturation state, coupled with the increase in partial pressure of CO₂ (pCO₂), of subsurface coastal waters over time from the combined effects of acidification and respiration processes represents a developing and, in some cases, present-day threat to calcifying and non-calcifying marine organisms across the range of different life stages, taxa and habitats (Orr et al., 2005; Fabry et al., 2008; Feely et al., 2004, 2008, 2016; Guinotte and Fabry, 2008; Doney et al., 2009a, 2009b; Doney, 2010; Hofmann and Todgham, 2010; Lischka et al., 2011; Barton et al., 2012, 2015; Gruber et al., 2012; Hettinger et al., 2012; Hauri et al., 2013; Mackas and Galbraith, 2012; Manno et al., 2012; Kroeker et al., 2013; Frieder et al., 2014; Bednaršek et al., 2014, 2016; Gattuso and Hansson, 2011; Gattuso et al., 2015a; Waldbusser et al., 2015; Somero et al., 2016; Weisberg et al., 2016). Acidification of surface waters, resulting from the oceanic uptake of approximately 28% of the global anthropogenic carbon dioxide emissions has caused a lowering of average surface water pH by about 0.11 units and 0.5 units in aragonite saturation state (Feely et al., 2004, 2009, 2012; Gattuso et al., 2015a). Oxidative breakdown of organic matter sinking through the water column in subsurface waters can further reduce the pH and aragonite and calcite saturation state via respiration processes which are often enhanced in highly productive estuarine and coastal waters (Fig. 1c). How these processes interact and are impacted by changing temperature, salinity, gas solubility, and carbonate chemistry has been explored for pH and calcite saturation state for the Gulf of Mexico, East China Sea, and Baltic Sea (Cai et al., 2011; Sunda and Cai, 2012; Laurent et al., 2017).

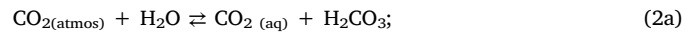
Increased acidification and hypoxia are related because aerobic respiration of organic matter consumes oxygen and produces CO₂ in approximate stoichiometric equivalence (Redfield et al., 1963):



Thus, processes that create subsurface oxygen deficits can also exacerbate acidifying conditions for marine organisms. Here we build upon earlier work and compare the results of our recent studies of the chemical composition of surface and subsurface waters from the coastal

waters of the California Current Ecosystem with previously published data from the Gulf of Mexico to show how significant differences in gas solubility, Revelle factor, and temperature affect in-situ chemical conditions in the water column of a cold-water upwelling coastal environment.

As atmospheric CO₂ increases and equilibrates with seawater, hydrogen ion (H⁺) and bicarbonate (HCO₃⁻) is produced and carbonate ion (CO₃²⁻) is consumed via a series of chemical reactions:



where

$$K_0^* = ([CO_{2(aq)}] + [H_2CO_3])/pCO_2 \quad (2b)$$



where

$$K_1^* = [H^+][HCO_3^-]/([CO_{2(aq)}] + [H_2CO_3]) \quad (3b)$$



where

$$K_2^* = [H^+][CO_3^{2-}]/[HCO_3^-] \quad (4b)$$



where

$$K_{sp}^* = [Ca^{2+}][CO_3^{2-}]. \quad (5b)$$

The air-sea CO₂ exchange reaction (2) leads to an initial increase in dissolved CO₂ in surface waters from gas exchange. The dissolved CO₂ reacts with H₂O to form carbonic acid (2). A portion of the carbonic acid quickly dissociates into a hydrogen ion and a bicarbonate ion (3), with K₁^{*} being the dissociation constant for (3). The bicarbonate ion can dissociate into a hydrogen ion and a carbonate ion (4), and K₂^{*} is the dissociation constant for (4). In addition, dissolved calcium (Ca²⁺) can combine with CO₃²⁻ to form a calcium carbonate (CaCO₃) mineral such as aragonite or calcite (5), with K_{sp}^{*} being the stoichiometric solubility product at saturation for calcium carbonate. The net result is

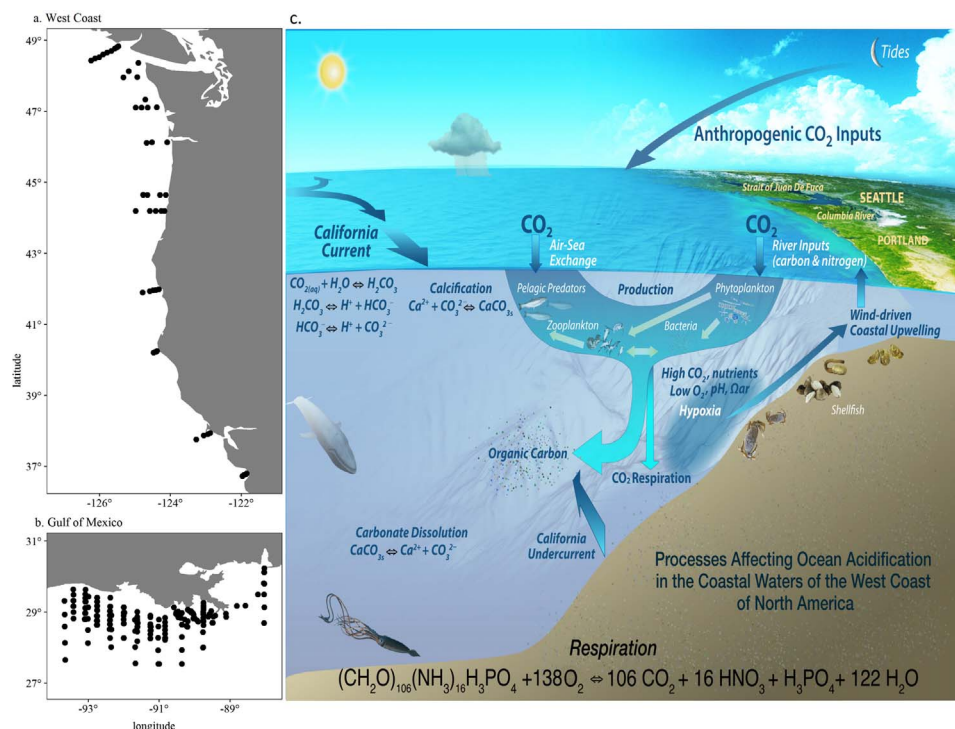
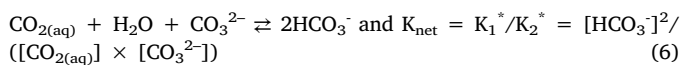


Fig. 1. Coastal sampling stations along: (a) West Coast of North America in summer of 2013; (b) northern Gulf of Mexico from 2006 to 2009; and (c) schematic diagram of physical and biogeochemical processes involved.

that the addition of CO₂ from the atmosphere leads to overall increases in hydrogen ion and bicarbonate and decreases in carbonate ion as is illustrated below in a combined equation:



Another important factor related to the carbonate chemistry is the efficiency with which the oceans can continue to absorb more CO₂ from the atmosphere and convert it to dissolved inorganic carbon (DIC), which is the sum of all carbonate species concentrations in $\mu\text{mol kg}^{-1}$. This efficiency is defined as the Revelle Factor (RF):

$$\text{RF} = (\Delta p\text{CO}_2/p\text{CO}_2)/(\Delta\text{DIC}/\text{DIC}); \quad (7)$$

where $p\text{CO}_2$ is the CO₂ partial pressure in μatm . In ocean surface waters, the RF generally ranges from 8 to 18, with the lower values in warm subtropical waters and the higher values in the cold high-latitude regions (Sabine et al., 2004; Sabine and Tanhua, 2010; Egleston et al., 2010). Note that higher RF indicates lower buffering capacity.

As the oceans take up more anthropogenic CO₂, the RF increases indicating that both the $p\text{CO}_2$ increase and pH_T (pH expressed in the total hydrogen ion concentration scale) decrease will be larger for each $1 \mu\text{mol kg}^{-1}$ increase in DIC. Consequently, we might also expect to see more extensive changes and higher seasonal variability of these parameters in colder less buffered waters.

In the late summer of 2013, we studied the extent of acidified conditions along the West Coast of North America from the coastal region off Washington, Oregon, and northern California. We conducted detailed chemical and hydrographic measurements in the region in order to better understand the relationships among these natural and human-induced processes that lead to acidification of the water column and their impact on pH_T and aragonite saturation. Some parts of the California Current Ecosystem are particularly vulnerable because of the combined effects of acidification, warming, upwelling, and hypoxia, which are enhanced in the late summer and early fall months when respiration-induced oxygen depletions are at their maximum extent (Hickey, 1979; Grantham et al., 2004; Hales et al., 2006; Feely et al., 2008, 2016; Chan et al., 2008, 2017; Rykaczewski and Dunne, 2010; Thomson and Krassovski, 2010; Booth et al., 2012; Harris et al., 2013; Siedlecki et al., 2016; Turi et al., 2016). Ocean acidification (OA) decreases the concentration of CO₃²⁻, presenting a challenge for many marine calcifiers (Eq. (5)). One measure of the thermodynamic favorability for the precipitation of CaCO₃ is saturation state. The saturation states of aragonite (Ω_{ar}) and calcite (Ω_{cal}) are a function of the concentrations of dissolved Ca²⁺ and CO₃²⁻, and the temperature and pressure-dependent stoichiometric solubility product,

$$\Omega_{\text{ar}} = [\text{Ca}^{2+}][\text{CO}_3^{2-}]/K_{\text{spar}}^* \quad (8)$$

$$\Omega_{\text{cal}} = [\text{Ca}^{2+}][\text{CO}_3^{2-}]/K_{\text{spscal}}^* \quad (9)$$

such that Ω_{ar} and Ω_{cal} will decline as more CO₂ is taken up by the oceans. At $\Omega = 1$, the carbonate minerals are in equilibrium with the surrounding seawater; at $\Omega > 1$, precipitation or preservation of carbonate minerals is thermodynamically favored; and at $\Omega < 1$, dissolution is favored (Mucci, 1983). The stoichiometric solubility products, K_{spar}^* and K_{spscal}^* , increase with increasing pressure and decreasing temperature such that as temperature decreases and/or pressure increases Ω_{ar} and Ω_{cal} decrease.

Although $\Omega = 1$ is commonly referenced as an abiotic threshold for CaCO₃ dissolution and precipitation, it is important to note that biogenic shell processes are not tightly bound to the $\Omega = 1$ threshold. Instead, decreases in dissolution and calcification occur at various Ω values. For example, depending on the organismal life stage, shell dissolution in various marine calcifiers can start at Ω values ranging from 1.3 to 1.6 (Bednaršek et al., 2014; Waldbusser et al., 2015), while shell calcification can also occur at Ω values < 1 (Comeau et al., 2010), although at much reduced level (Langdon and Atkinson, 2005;

Bednaršek et al., 2017). With decreasing Ω , organisms have to compensate against energetically more expensive processes and maintenance costs (O'Donnell et al., 2013; Wood et al., 2008).

While Ω predominantly affects marine calcifiers, $p\text{CO}_2$ as a stressor can negatively affect both calcifiers and non-calcifiers, subjecting them to the stress of hypercapnia. Hypercapnia is associated with the exposures of 1000 $\mu\text{atm } p\text{CO}_2$ for more than one month (McNeil and Sasse, 2016). Elevated $p\text{CO}_2$ and the attendant increased H⁺ concentrations in the extracellular space lead to changes in the acid-base balance and organismal internal acidosis. Hypercapnia exposure in lower marine invertebrates with poor capacity to compensate for pH change results in metabolic depression, reduced level of protein synthesis, and reduced growth. In fish, high CO₂ exposure interferes with neurotransmitter function, impaired olfactory sense, increased boldness, and loss of behavioral lateralization (Nilsson et al., 2012; Dixon et al., 2010), leading to overall impaired neurological and behavioral functioning. Ultimately, these disturbances can substantially increase the energetic costs of maintaining cellular homeostasis, resulting in physiological tradeoffs and shutting down some biological processes.

From a biological perspective, the US West Coast and Gulf of Mexico are two fundamentally different regimes with respect to surface water initial conditions that determine organismal exposure to OA. While the concentrations and values of biologically-relevant OA parameters in the Gulf of Mexico are much more favorable at present time, the OA conditions along the US West Coast have been demonstrated to already have a detrimental impact on some species (Bednaršek et al., 2014, 2017). Since hypercapnia is defined as the exposures of 1000 $\mu\text{atm } p\text{CO}_2$ for more than one month, some organisms are already experiencing chronic hypercapnia and low aragonite saturation state along the US West Coast. This condition is indicative of reduced habitat availability for some benthic and pelagic marine organisms, such as pteropods (Bednaršek et al., 2014, 2017; Feely et al., 2016) and oysters (Waldbusser et al., 2015; Hales et al., 2017). In contrast, there is no subsurface hypercapnic exposure in the Gulf of Mexico. It is important to emphasize that some taxa in the upwelling regimes are expected to have developed acclimatization-adaptation strategies over longer periods of time to allow them for coping with hypercapnia/low Ω exposure. On the other hand, in the absence of unfavorable conditions that would influence long-term development of adaptation capacity, the organisms in the Gulf of Mexico are predicted to have higher sensitivity to small scale changes in hypercapnic/OA stress in the near-future. In this paper, we will compare the changing pH_T and carbonate chemistry from the surface ocean to the hypoxic boundary ($\text{O}_2 \sim 60 \mu\text{mol kg}^{-1}$) for the West Coast of North America and Gulf of Mexico and examine how the two regions will evolve in the future under high-CO₂ conditions.

2. Sampling and analytical methods

Detailed observations of carbonate system chemistry and other physical and chemical parameters were made along the western North American continental shelf (Fig. 1a). Vertical profiles of temperature, conductivity and pressure were obtained with a Seabird SBE 911plus CTD. Water samples from this cruise were collected in modified Niskintype bottles and analyzed under ship-based or land-based laboratory conditions for DIC, total alkalinity (TA), pH_T , oxygen, and nutrients. DIC was measured by coulometric titration (Johnson et al., 1987; Dickson and Goyet, 1994; Ono et al., 1998), and TA was measured by the potentiometric titration method (Millero et al., 1993; Millero, 1995; Dickson and Goyet, 1994; Ono et al., 1998). Certified Reference Materials (CRM) were analyzed for DIC and TA as an independent verification of instrument calibrations (Dickson et al., 2007). The ship-based DIC and TA measurements each have a combined precision and accuracy within $2 \mu\text{mol kg}^{-1}$ ($\pm 0.1\%$). The spectrophotometric method described by Byrne et al. (2010) and Liu et al. (2011) was used

to measure pH on the total scale (pH_T). The saturation state of seawater with respect to aragonite was calculated from the DIC and TA data using the program CO2SYS developed by Lewis and Wallace (1998). The pressure effect on the solubility, for samples collected at depth, is estimated from the equation of Mucci (1983), incorporating adjustments to the constants recommended by Millero (1995). Based on the uncertainties in the DIC and TA measurements and the thermodynamic constants, the uncertainty in the calculated Ω_{ar} is approximately 0.02. Oxygen analysis was conducted by modified Winkler titration (Carpenter, 1965; which has an uncertainty of $\pm 1 \mu\text{mol kg}^{-1}$), and nutrients (nitrate, nitrite, ammonium, phosphate, silicate) were frozen at sea and analyzed using a Technicon AutoAnalyzer II (UNESCO, 1994) at Oregon State University.

The Gulf of Mexico data for this analysis were obtained during a series of cruises conducted in the northern Gulf of Mexico (Fig. 1b) from 2006 to 2009. These included four cruises on the U.S. Environmental Protection Agency Ocean Survey Vessel *Bold* during 6–11 June 2006, 6–11 September 2006, 2–8 May 2007, and 18–24 August 2007, focusing largely on the area of recurrent hypoxia in the northern Gulf of Mexico (cf. Huang et al., 2015). Additional shelf-wide cruises were conducted on the R/V *Cape Hatteras* 8–20 January 2009, 19 April–1 May 2009, 18–30 July 2009, 10–22 March and 28 October–9 November 2009 on the R/V *Sharp*. These cruises were selected because they covered a large portion of the study area and encompassed inner to outer shelf water-mass regimes.

In the Gulf of Mexico, water samples were taken from Niskin bottles into 250 mL borosilicate glass bottles and were poisoned with saturated HgCl_2 solution immediately after sampling and were kept in low temperature ($\sim 5^\circ\text{C}$) until being analyzed in the laboratory (within five weeks of sample collection). DIC was measured with an infrared CO_2 detector-based DIC analyzer (AS-C3 Apollo Scitech). TA was measured with the open-cell Gran titration method using a temperature-controlled, semi-automated titrator (AS-ALK2 Apollo Scitech). Both TA and DIC measurements were directly referenced to CRM. TA and DIC measurements had precision and accuracy of $\pm 0.1\%$ (Cai et al., 2010; Huang et al., 2012).

3. Modeling

Procedures for estimating changes in carbonate chemistry follow Cai et al. (2011) and Sunda and Cai (2012). Briefly, saturated dissolved oxygen concentrations of surface waters (pressure (P) < 15 dbar) were calculated as a function of temperature and salinity for the West Coast and Gulf of Mexico. The initial carbonate chemistry for surface waters was calculated using DIC and TA. Atmospheric $p\text{CO}_2$ was set at five levels (400, 430, 550, 750, and 910 ppm) corresponding to present-day and year 2100 Representative Concentration Pathway (RCP) scenarios 2.6, 4.5, 6.0, and 8.5 (van Vuuren et al., 2011; IPCC, 2013; Table 1). Once the initial surface conditions were calculated, aerobic oxidation was assumed to increase DIC in subsurface waters due to respiration at the Redfield ratio of 106 CO_2 to 138 O_2 (Redfield et al., 1963). The final

DIC was used to calculate the carbonate chemistry assuming constant TA, temperature, salinity, and pressure to facilitate comparisons with surface waters.

All calculations were performed using the *seacarb* v3.0.14 (Gattuso et al., 2015b) and *marelac* v2.1.5 (Soetaert et al., 2015) packages in R v3.3.1 (R Core Team, 2016a, 2016b) using equilibrium constants K_1^* and K_2^* from Lueker et al. (2000), K_{HSO_4} from Dickson (1990a); $K_{\text{B(OH)}_3}$ from Dickson (1990b); $K_{\text{H}_3\text{PO}_4}$, $K_{\text{H}_2\text{PO}_4}$, K_{HPO_4} , $K_{\text{H}_2\text{O}}$, and K_{Si} from Millero (1995); and K_F from Perez and Fraga (1987). Carbonate alkalinity was calculated from the total alkalinity in conjunction with total concentrations of boron (Uppström, 1974), sulfur (Morris and Riley, 1966), and fluoride (Riley, 1965) in direct proportion to salinity. Since their effects are relatively small, phosphate and silicate concentrations were assumed to be $0 \mu\text{mol kg}^{-1}$ for the model calculations.

4. Cruise results

At all depths, the mean temperature, salinity, and aragonite saturation values in the Gulf of Mexico are significantly higher than the West Coast (Fig. 2). In contrast, Gulf of Mexico the mean dissolved oxygen was as much as 50% lower in the upper 20–30 m while pH_T below 40 m is lower in West Coast waters. The 2013 West Coast cruise results showed evidence that surface seawater was close to equilibrium with respect to CO_2 in the atmosphere in most regions, except for the nearshore upwelling region along the coast. Lowest pH_T values (< 8.0) occurred in waters near the mouth of the Columbia River and to the south along the Oregon coast (Fig. 3). Farther offshore, oxygen concentrations are high ($> 250 \mu\text{mol kg}^{-1}$), and surface pH_T values quickly increase to open-ocean values ranging from 8.0 to 8.2 with aragonite saturation values ranging from 2.0 to 2.6. The West Coast subsurface oxygen data show evidence for a large respiration signal in the near-coastal region, with O_2 concentrations dropping below the hypoxic threshold ($< 60 \mu\text{mol kg}^{-1}$) in nearshore and mid-shelf regions of Washington and Oregon. Correspondingly, the pH_T and aragonite saturation data show evidence for extremely low values (< 7.6 and < 0.6 , respectively) at the same locations and depths. The data from the West Coast cruise and the northern Gulf of Mexico indicate a significant positive linear correlation between pH_T with dissolved oxygen in subsurface waters (Fig. 4a).

The results from both data sets suggest that the respiration signal below the surface enhances water column acidification via organic matter oxidation (i.e., oxidative acidification). Aragonite saturation is also positively correlated with dissolved oxygen but there is more curvature in the results (Fig. 4b). Of particular note is the fact that while the initial surface pH_T values are quite similar for both regions the aragonite saturation state initial conditions are very different, with the Gulf of Mexico data showing higher initial aragonite saturation state values than the West Coast data. At the low-oxygen end of the plot the Gulf of Mexico data show consistently higher pH_T and aragonite saturation values than the West Coast data. These results indicate that initial conditions play a significant role in the overall biogeochemical

Table 1

Effect of increasing atmospheric CO_2 on carbonate system parameters in surface seawater for the US West Coast and northern Gulf of Mexico in year 2100, assuming constant temperature, salinity, initial oxygen concentration, and alkalinity.

Location	RCP	T ($^\circ\text{C}$)	S	O_2 ($\mu\text{mol kg}^{-1}$)	$p\text{CO}_{2\text{atm}}$ (ppm)	$p\text{CO}_{2\text{sw}}$ (μatm)	TA ($\mu\text{mol kg}^{-1}$)	DIC ($\mu\text{mol kg}^{-1}$)	pH	CO_3^{2-} ($\mu\text{mol kg}^{-1}$)	Ω_{ar}	Ω_{cal}	RF
West Coast	0	11.8	32.7	265	400	395	2218	2042	8.043	130	2.00	3.14	12.7
West Coast	2.6	11.8	32.7	265	430	424	2218	2053	8.015	123	1.89	2.98	13.2
West Coast	4.5	11.8	32.7	265	550	543	2218	2090	7.920	102	1.56	2.46	14.6
West Coast	6	11.8	32.7	265	750	740	2218	2132	7.798	79	1.21	1.91	16.5
West Coast	8.5	11.8	32.7	265	910	898	2218	2156	7.720	67	1.03	1.62	17.5
Gulf of Mexico	0	26.7	33.3	200	400	386	2389	2062	8.074	238	3.84	5.82	9.4
Gulf of Mexico	2.6	26.7	33.3	200	430	415	2389	2077	8.048	227	3.68	5.57	9.7
Gulf of Mexico	4.5	26.7	33.3	200	550	531	2389	2128	7.960	194	3.13	4.75	10.6
Gulf of Mexico	6	26.7	33.3	200	750	725	2389	2188	7.846	156	2.52	3.82	12.0
Gulf of Mexico	8.5	26.7	33.3	200	910	879	2389	2222	7.773	135	2.19	3.31	13.1

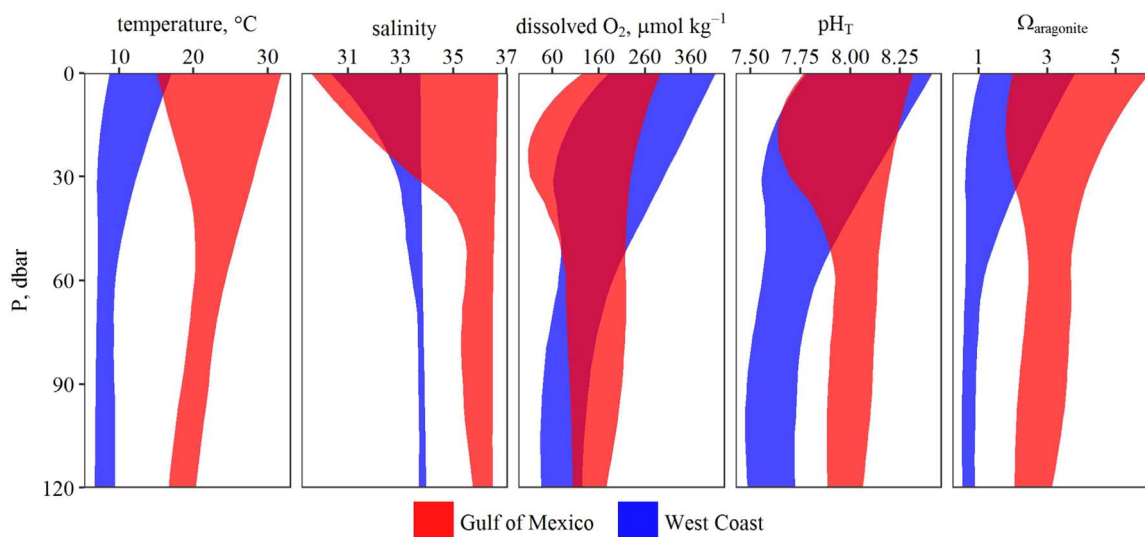


Fig. 2. Composite vertical profiles (range of observations for each depth) of temperature, salinity, oxygen, pH_T , and aragonite saturation state for the northern Gulf of Mexico (red) and U.S. West Coast (blue). (For interpretation of the references to color in this figure legend, the reader is referred to the web version of this article).

changes that take place in the water column as a water mass leaves the surface mixed layer and respiration processes begin to alter subsurface carbonate system properties. The Gulf of Mexico O_2 saturation values, which range from approximately 180 to 225 $\mu\text{mol kg}^{-1}$, are typical of warm, salty subtropical waters; whereas the West Coast O_2 saturation values are approximately 20–100 $\mu\text{mol kg}^{-1}$ higher because the waters are cooler and less saline (Fig. 4c). This means that lowering oxygen concentrations down to hypoxic levels in West Coast waters requires more remineralization of organic carbon than for subsurface waters of the Gulf of Mexico. Assuming organic matter is not limiting, increased respiration of organic matter due to higher initial O_2 concentration, and perhaps longer subsurface water column retention time, leads to more carbon dioxide production, which results in a greater reduction of in situ pH_T in the colder, West Coast waters.

Increasing atmospheric $p\text{CO}_2$ from present-day (400 μatm) to the RCP 8.5 value of 910 μatm in year 2100 will decrease the pH_T of initial surface waters by approximately 0.3 pH units in both the West Coast and Gulf of Mexico and will decrease Ω_{ar} by 1.0 and 1.7 units, respectively. For comparison, at RCP 4.5 (550 μatm atmospheric $p\text{CO}_2$) the pH_T decrease from initial conditions would be about 0.12 for both regions and the Ω_{ar} decrease would be about 0.44 and 0.71, respectively, for the West Coast and Gulf of Mexico. Furthermore, dissolved oxygen will only decline by about 1.5–2% with each 1 °C increase in temperature, translating to 8–13 $\mu\text{mol kg}^{-1}$ less CO_2 at the hypoxia threshold assuming surface waters warm 3 °C (Khan et al., 2013). Between the two coastal regimes, the higher dissolved oxygen pool in the colder West Coast waters predisposes the West Coast to larger increases in dissolved CO_2 relative to the Gulf of Mexico as organic matter is remineralized in the water column. However, the modeled current and future changes in carbonate chemistry of the two regions illustrate a decoupling of pH_T and Ω_{ar} responses to increasing CO_2 . Currently, from the surface to the hypoxic zone, pH_T decreases by 0.47 and 0.19 pH units, respectively, for the West Coast and Gulf of Mexico, whereas Ω_{ar} decreases by 1.25 and 1.13 units, respectively. Under RCP 8.5 in year 2100, the pH_T decreases are 0.51 and 0.28 pH units, while Ω_{ar} decreases are 0.69 and 0.95 units respectively. In other words, future subsurface declines in pH_T are about the same as present-day for the West Coast but are proportionately more extreme for the Gulf of Mexico; whereas future Ω_{ar} declines are less extreme for both West Coast and the Gulf of Mexico. Consequently, oxidative acidification changes in the entire carbonate system vary as a function of the initial surface conditions, including the atmospheric CO_2 concentration.

5. Comparison of the effects of anthropogenic CO_2 on present and future acidification conditions in West Coast and Gulf of Mexico coastal waters

With increasing anthropogenic CO_2 emissions over the next several decades, both pH_T and aragonite saturation state are expected to decrease in surface and subsurface coastal waters and $p\text{CO}_2$ will increase. At the surface, the percentage change in the carbon parameters are very similar for both regions even though the absolute change in aragonite saturation is much higher in the warmer waters of the Gulf of Mexico. For example, Table 1 and Figs. 4–8 show comparisons of the expected changes in average pH_T , aragonite saturation and $p\text{CO}_2$ of surface waters from the West Coast and Gulf of Mexico as they are subjected to increased CO_2 emissions. With respect to surface seawater pH_T , the decrease from present-day to RCP 8.5 is 0.32 units (from 8.04 to 7.72) in West Coast waters as compared with 0.30 units (from 8.07 to 7.77) for the Gulf of Mexico waters. These decreases correspond to increases in $[\text{H}^+]$ of 110% and 100%, respectively. At a maximum RCP of 8.5 the surface aragonite saturation decrease is about 48% (from 2.00 to 1.03) in West Coast waters as compared with 43% (from 3.84 to 2.19) for the Gulf of Mexico (Table 1). For surface seawater $p\text{CO}_2$ the increase from present-day to RCP 8.5 is approximately 130% for both systems (Table 1).

On the other hand, when a seawater parcel sinks below the surface via mixing or lateral transport and undergoes aerobic respiration down to the hypoxic boundary, acidification will be enhanced to a different degree at the two locations depending on the initial starting carbon system conditions, oxygen concentrations, temperature, and salinity. In particular, chemical changes in subsurface waters are magnified due to the differences in initial oxygen concentrations and decreases in the buffer capacity (i.e., increasing RF) with decreasing oxygen concentration. Under present day conditions, oxidation-driven increases in CO_2 result in pH_T decreases of 0.46 units from 8.04 at the surface to 7.58 at the hypoxic boundary in West Coast waters and 0.19 units (from 8.07 to 7.88) in the Gulf of Mexico (Tables 1 and 2; Figs. 5 and 6). These pH_T decreases correspond to increases in $[\text{H}^+]$ of 194% and 55% from the surface to the hypoxic boundary, respectively for the West Coast and Gulf of Mexico. The oxidation-driven chemistry changes are further amplified under RCP 8.5 with pH_T declining from the surface by 0.51 units (7.72 to 7.21) and 0.27 units (7.77 to 7.50) in West Coast and Gulf of Mexico waters, respectively (Tables 1, 2). These declines correspond to increases in $[\text{H}^+]$ of 223% and 89%, respectively (Tables 1 and 2; Fig. 5).

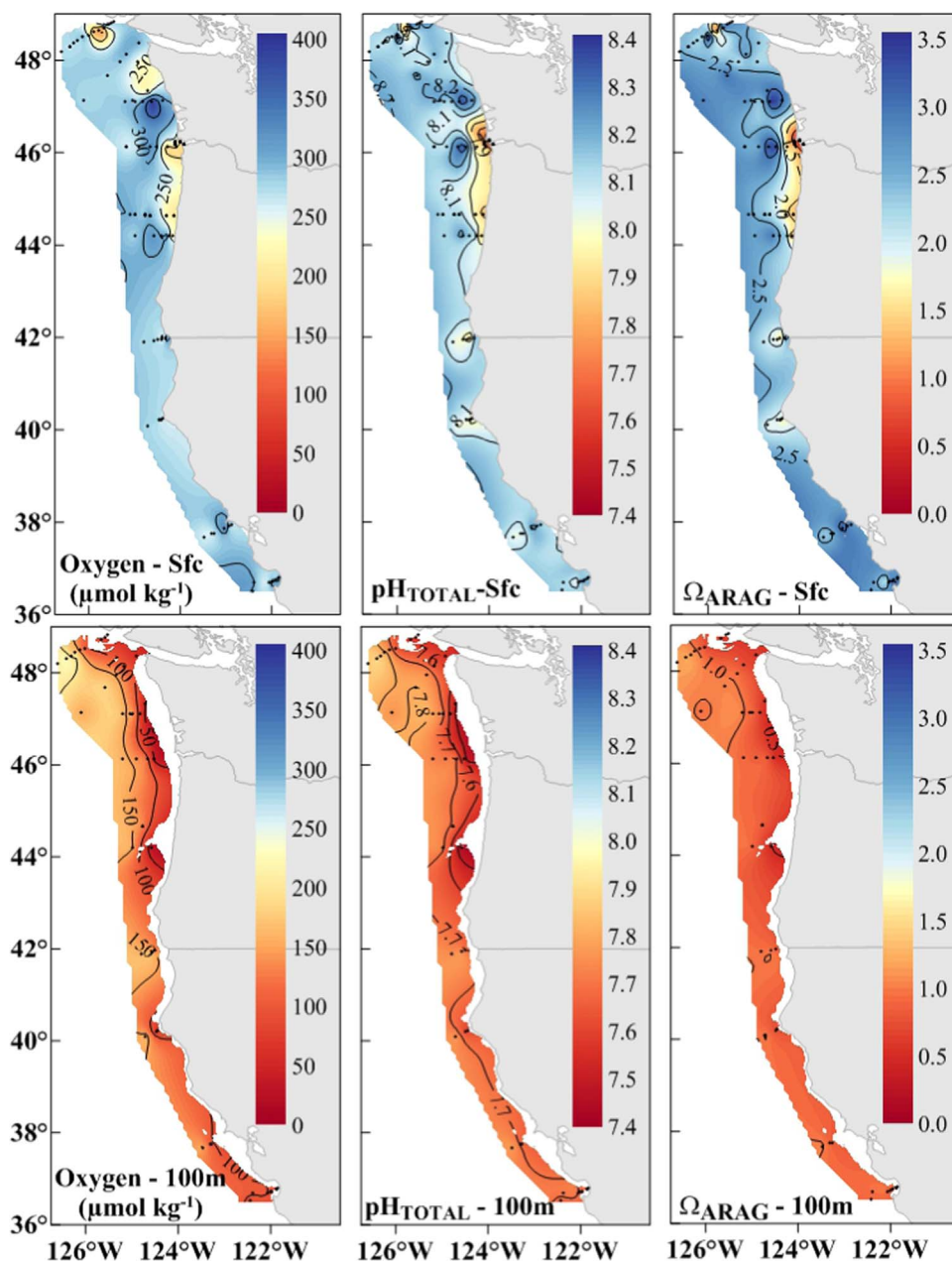


Fig. 3. Distributions of dissolved oxygen in $\mu\text{mol kg}^{-1}$, in situ pH_T , and aragonite saturation state at the surface (top panel) and 100 m (bottom panel) for the 2013 West Coast cruise (5–26 August 2013).

For aragonite saturation state, the oxidation-driven changes are also further amplified under RCP 8.5 with aragonite saturation declining from the surface by 67% (1.0 to 0.3) in the West Coast and 45% (2.2 to 1.2; Tables 1 and 2) in the Gulf of Mexico. Under present-day conditions and also under RCP 8.5, respiration-driven increases in CO_2 result in aragonite saturation state declines that are nearly identical to the percent changes in the CO_3^{2-} ion concentration. Similarly, the pCO_2 is also enhanced at the hypoxic boundary under RCP 8.5 with an increase from present-day to RCP 8.5 equal to 139% 1283–3060 μatm for the West Coast and 170% 655–1770 μatm for the Gulf of Mexico.

The agreement between the discrete pH_T and Ω_{ar} data and the model contours for different temperatures (Fig. 4a,b) suggests that oxidation of organic matter (i.e., the oxidative acidification) drives the decrease in pH_T (Fig. 5) and saturation state (Fig. 6), as well as the increases in pCO_2 (Fig. 7) and RF (Fig. 8), with depth in the subsurface waters. The magnitude of the declines in pH_T and aragonite saturation state are determined by the minor carbon species that have the largest effect on those parameters, namely dissolved CO_2 and CO_3^{2-} , respectively. The oxidation of organic matter consumes oxygen and produces

CO_2 , thus increasing subsurface pCO_2 . Increased CO_2 reacts with H_2O to form carbonic acid, which reacts with CO_3^{2-} to form HCO_3^- , steadily decreasing pH_T as the pool of CO_2 increases (Eq. (2)). Consequently, pH_T and dissolved oxygen concentrations have a largely linear relationship (Fig. 4a). The CO_3^{2-} concentration largely determines the saturation states of aragonite (Eqs. (8) and (9); Fig. 6). As the addition of protons to the water column titrates CO_3^{2-} , the pool of $[\text{CO}_3^{2-}]$ diminishes and aragonite saturation state declines (Fig. 8).

6. Discussion

Bjerrum plots of the carbonate species changes illustrate how the two ocean locations can be expected to respond under high- CO_2 emissions (Fig. 9). Colder oceans with greater initial dissolved oxygen concentrations (e.g., the West Coast) experience larger increases in CO_2 from surface to the hypoxic boundary and therefore have greater shifts to the left along the pH_T scale of the Bjerrum diagram (Fig. 9a, b). This demonstrates how both waters start at similar pH conditions at the surface (Table 1, Figs. 4a, 5a, b) but colder waters experience larger

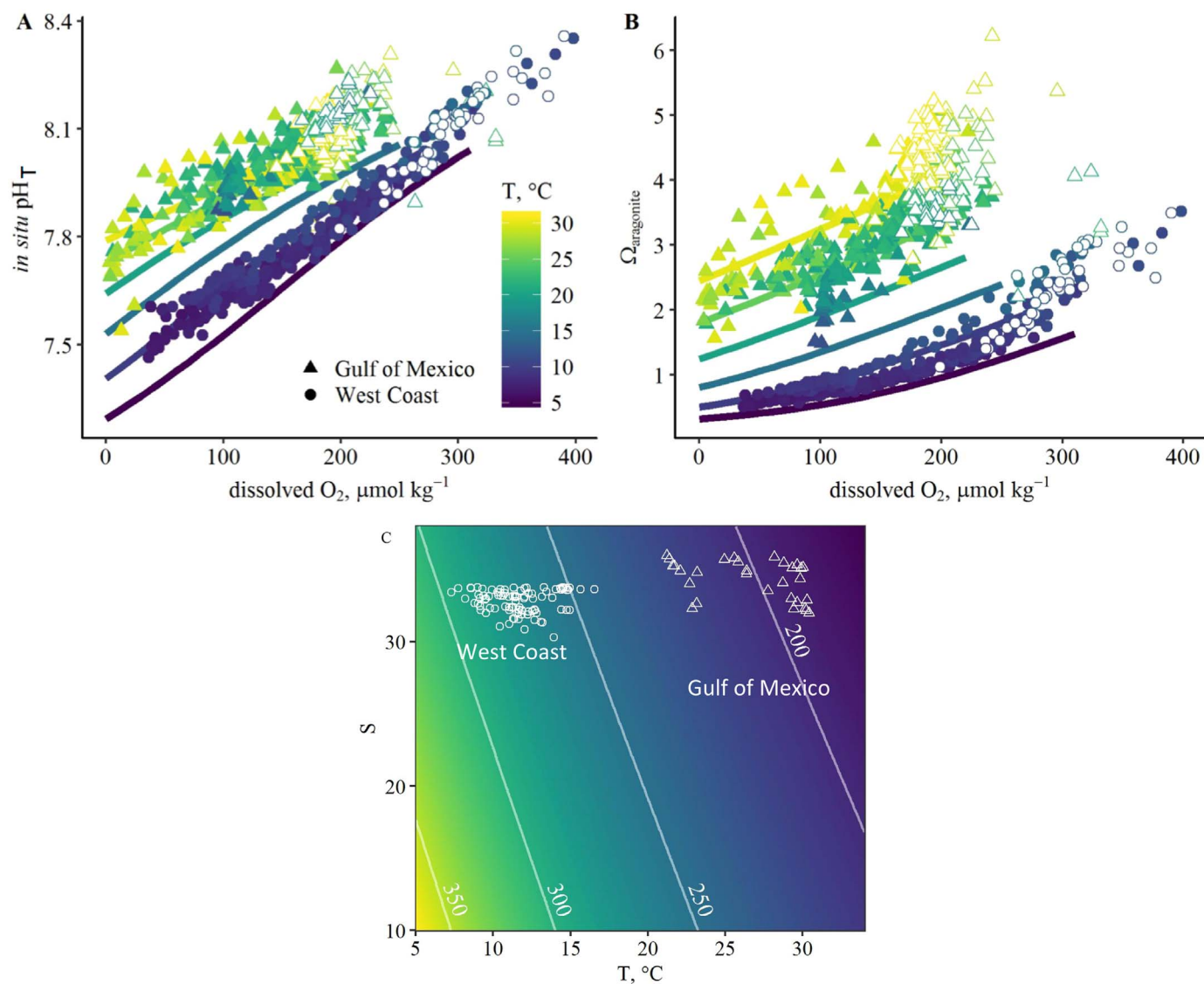


Fig. 4. Plots of: (a) in situ pH_T ; (b) aragonite saturation state as function of dissolved oxygen in $\mu\text{mol kg}^{-1}$. Lines represent modeled changes in chemistry due to oxidation at 5°C increments where $S = 33.5$ and $\text{TA} = 2300 \mu\text{mol kg}^{-1}$. The right end of each model line represents surface conditions where oxygen is in equilibrium with the atmosphere at 400 ppm CO_2 . Points represent cruise data for the Gulf of Mexico (triangles) and West Coast (circles) at the surface (open symbols, $P < 12 \text{ dbar}$ or 15 dbar for West Coast and Gulf of Mexico, respectively) and subsurface (solid symbols); and c) surface oxygen saturation concentrations in $\mu\text{mol kg}^{-1}$ for typical salinity and temperature values observed in the Gulf of Mexico (open triangles) and US West Coast (open circles). The contours are lines of constant O_2 concentration in $\mu\text{mol kg}^{-1}$.

pH_T declines at depth (Fig. 6a, b). As pH_T declines along the Bjerrum diagram past the HCO_3^- peak, CO_3^{2-} is depleted (Fig. 9a, b), and more carbon remains as dissolved CO_2 as the DIC pool increases. The dissolved CO_2 distributions indicate a shift from a system where dissolved CO_2 is the least abundant DIC species in the present-day to one where CO_3^{2-} has a lower concentration than dissolved CO_2 in RCP 8.5. With increasing atmospheric CO_2 , the shift will occur sooner in the colder West Coast water than the warmer northern Gulf of Mexico water (Sunda and Cai, 2012). Essentially, in the West Coast surface water, the CO_3^{2-} neutralization capacity is already lower at present-day but this capacity will be nearly depleted at RCP8.5 condition, as shown by the relative positions of the arrow tails between CO_3^{2-} and CO_2 in Fig. 9b. Therefore, under RCP8.5 the water along the West Coast will not have much buffering capacity for neutralizing CO_2 released from respiration. In contrast, there is a much stronger buffering capacity in the Gulf of Mexico surface water, and it will last through the RCP8.5 condition.

As anthropogenic CO_2 concentrations begin to build up in subsurface waters, increased atmospheric CO_2 will expose organisms to hypercapnia within subsurface depths (Reum et al., 2016; McNeil and

Sasse, 2016). The timing and extent of this subsurface exposure will occur sooner and be more widespread in colder surface and subsurface waters. This phenomenon is a result of the changing initial carbonate chemistry and increasing RF with increasing DIC (Tables 1 and 2). In ecosystems with high RF the hypercapnia effects will be magnified and accelerated compared to the ecosystems with low RF. In this case, oceanic waters along the US West Coast will reach critical thresholds for hypercapnia much earlier, imposing negative effects to numerous groups of organisms and fish. The hypercapnic boundary occurs at 7.68 pH_T units in the U.S. West Coast and 7.72 pH_T units in the Gulf of Mexico. Currently, organisms in the West Coast are exposed to these conditions when oxygen concentrations are near $100 \mu\text{mol kg}^{-1}$ but will experience hypercapnia at oxygen concentrations of about $250 \mu\text{mol kg}^{-1}$ under RCP 8.5 conditions. Hypercapnia does not occur at present in the Gulf of Mexico but will occur at oxygen concentrations of $170 \mu\text{mol kg}^{-1}$ under RCP 8.5 conditions.

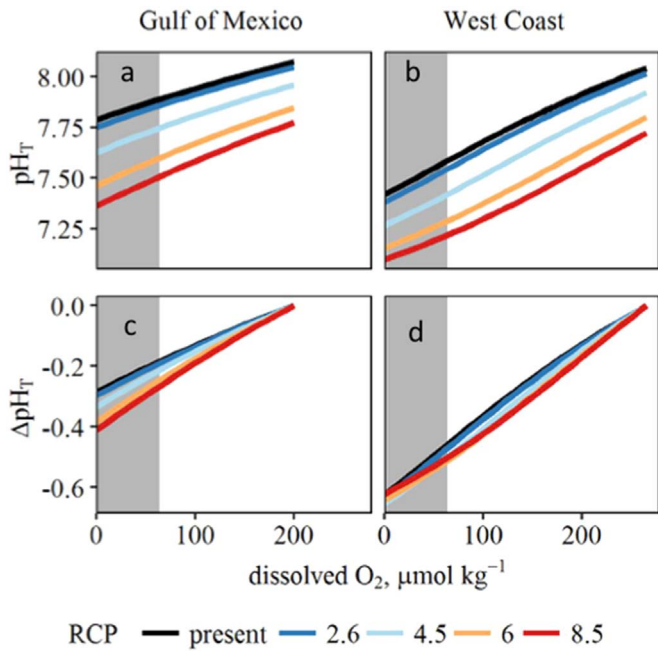


Fig. 5. In-situ pH_T (a and b) and ΔpH_T (c and d) as a function of dissolved oxygen concentration for different RCP CO₂ emission scenarios for average data from the Gulf of Mexico (a and c) and West Coast stations (b and d). The ΔpH_T is the change from the initial present-day surface water conditions. The shaded grey area represents the region of hypoxia.

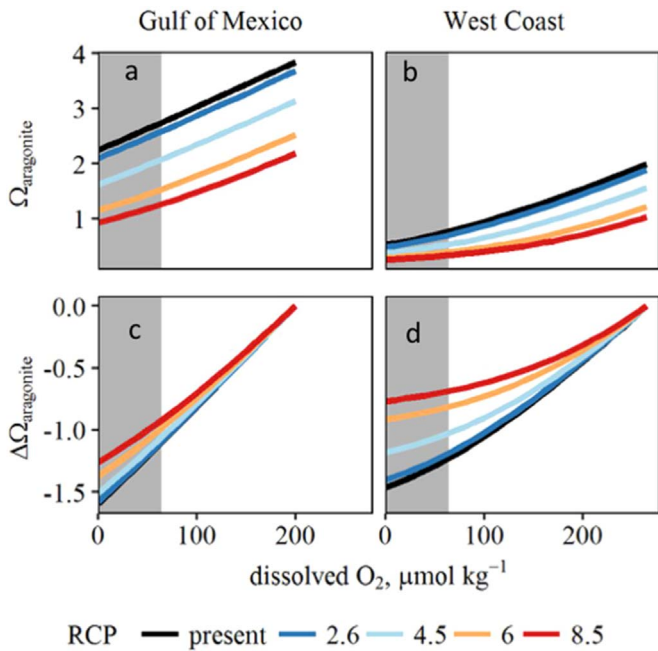


Fig. 6. Aragonite saturation state (Ω_{ar}) (a and b) and ΔΩ_{ar} from initial surface conditions (c and d) as a function of dissolved oxygen concentration for different RCP CO₂ emission scenarios for average data from the Gulf of Mexico (a and c) and West Coast stations (b and d). The ΔΩ_{ar} is the change from the initial present-day surface water conditions. The shaded grey area represents the region of hypoxia.

7. Biological effects of hypercapnia and other stressors

In the ecosystem with high RFs (US West Coast), which results in high non-linear pCO₂ amplification, the hypercapnia effects will be magnified and accelerated compared to the system with lower RFs (Gulf of Mexico). As such, oceanic waters along the US West Coast will reach critical thresholds for hypercapnia much sooner, imposing negative

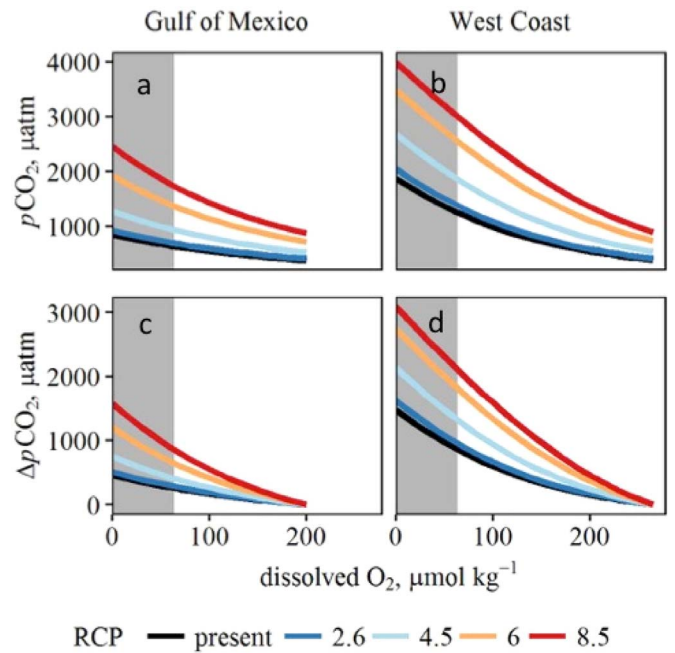


Fig. 7. Seawater pCO₂ (a and b) and ΔpCO₂ (c and d) as a function of dissolved oxygen concentration for different RCP CO₂ emission scenarios for average data from the Gulf of Mexico (a and c) and West Coast stations (b and d). The ΔpCO₂ is the change from the initial present-day surface water conditions. The shaded grey area represents the region of hypoxia.

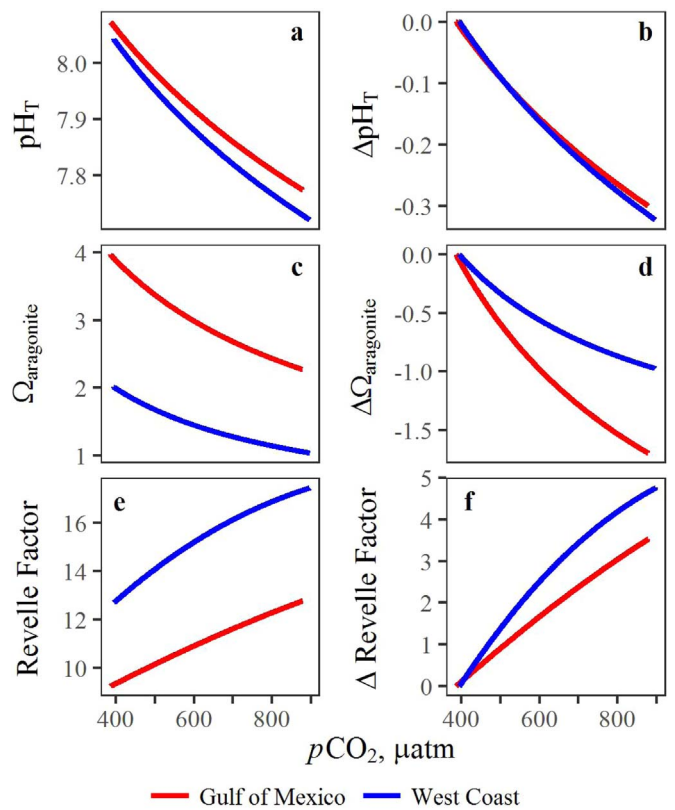


Fig. 8. Absolute and relative changes in seawater pH_T (a and b), aragonite saturation (c and d), and Revelle Factor (e and f) as a function of pCO₂ for average data from the Gulf of Mexico and West Coast. The relative changes are from the initial present-day surface water conditions.

effects to numerous groups of organisms and commercial fisheries. High Revelle factor-enhanced hypercapnia is especially vulnerable for the

Table 2
Carbonate conditions at the hypoxia threshold ($60 \mu\text{mol kg}^{-1}$ oxygen) from respiration-driven increases in CO_2 , starting from the initial surface conditions in Table 1.

Location	RCP	$p\text{CO}_{2\text{sw}}$ (μatm)	DIC ($\mu\text{mol kg}^{-1}$)	pH	CO_2 ($\mu\text{mol kg}^{-1}$)	HCO_3^- ($\mu\text{mol kg}^{-1}$)	CO_3^{2-} ($\mu\text{mol kg}^{-1}$)	Ω_{ar}	Ω_{cal}	RF
West Coast	0	1283	2199	7.575	54	2097	49	0.75	1.18	18.5
West Coast	2.6	1413	2211	7.535	59	2107	45	0.69	1.08	18.5
West Coast	4.5	1907	2247	7.410	80	2134	34	0.52	0.82	17.7
West Coast	6	2606	2289	7.279	109	2155	25	0.39	0.62	15.8
West Coast	8.5	3060	2314	7.211	128	2164	22	0.34	0.53	14.6
Gulf of Mexico	0	655	2169	7.883	18	1983	168	2.71	4.11	11.6
Gulf of Mexico	2.6	713	2185	7.852	20	2007	158	2.55	3.87	12.0
Gulf of Mexico	4.5	957	2236	7.740	26	2083	127	2.05	3.10	13.5
Gulf of Mexico	6	1399	2295	7.591	38	2164	93	1.51	2.29	15.5
Gulf of Mexico	8.5	1770	2329	7.497	48	2204	77	1.24	1.88	16.5

open ocean where pelagic habitats are not generally characterized by the same amount of natural variability in OA conditions as the coastal waters. This situation imposes high risk factors for the pelagic organisms with no previous acclimatization or adaptation to hypercapnia or low acid-base regulation, especially in the Gulf of Mexico. However, the absolute changes in oxygen concentrations, $p\text{CO}_2$, Ω and Revelle factors under high RCP scenarios are probably sufficient to impose physiological and behavioral impairments for lower marine invertebrates as well as for some fishes with lower tolerance to small changes in chemical conditions.

In addition, calcifiers also face the combined stressors of both hypercapnia and the shoaling of the aragonite saturation horizon, i.e. where saturation state = 1, corresponding to pH_T levels of 7.7 and 7.4 for the West Coast and Gulf of Mexico, respectively. The oxygen concentrations associated with saturation states of 1 are similar to those associated with hypercapnia for the US West Coast: $110 \mu\text{mol kg}^{-1}$ at present and $260 \mu\text{mol kg}^{-1}$ under RCP 8.5. In the Gulf of Mexico, the aragonite saturation horizon occurs at oxygen concentrations of about $15 \mu\text{mol kg}^{-1}$ under the RCP 8.5 conditions.

Comparing the two ecosystems under the most severe RCP 8.5

scenarios, the large change in amplitude of hypercapnia indicates the probability of extensive habitat compression along the US West Coast, while the conditions in the Gulf of Mexico will be undergoing slower degradation. Nevertheless, the Gulf of Mexico will continue to provide habitats that are suitable for numerous calcifying and non-calcifying species. While the direction of change is similar for both regions, the onset of key thresholds and the overall vulnerability will be felt more quickly in the cold-water regime of the West Coast. Since various OA parameters affect multiple impairment pathways, overlapping OA parameters actually represent multiple-stressor environments for marine organisms. This is especially important for the most sensitive organisms with low capacity for acid-base regulation.

8. Conclusions

The decrease in pH_T and aragonite saturation state, as well as the increase in $p\text{CO}_2$ of subsurface coastal waters, from the combined effects of “classical” ocean acidification and oxidative acidification (i.e., respiration processes) is significantly enhanced by the higher RF and the enhancement of the respiration process in the colder waters of the

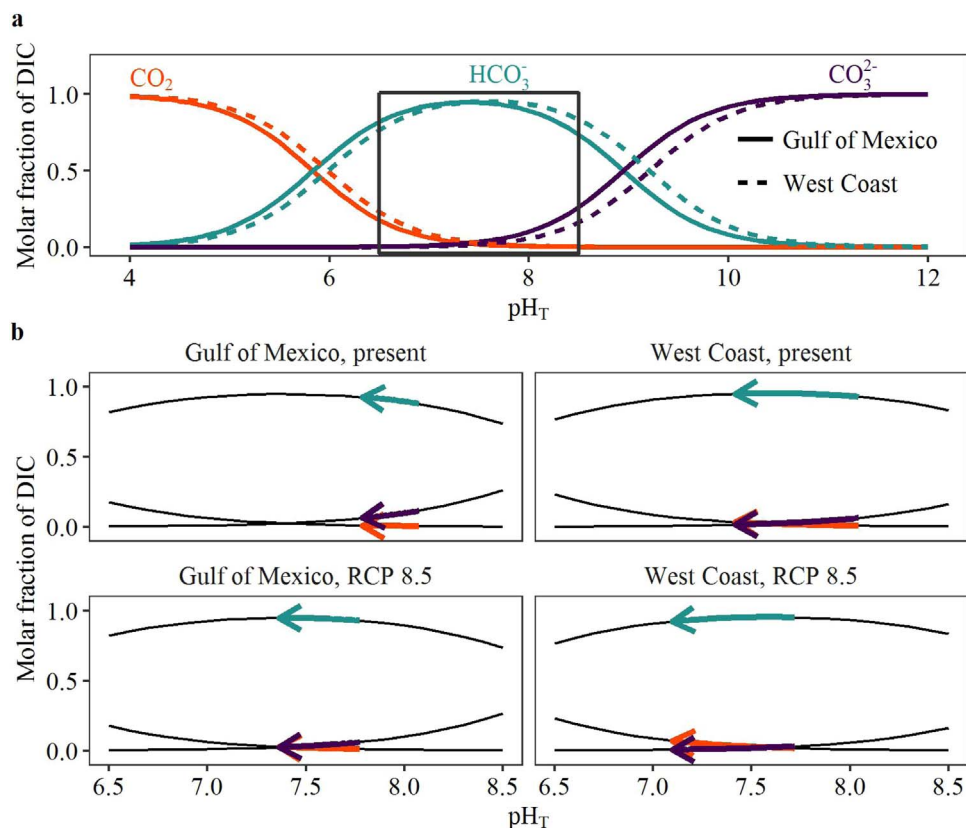


Fig. 9. Bjerrum plots of the changes in chemical speciation of the carbonate system with increasing CO_2 concentrations for the Gulf of Mexico and US West Coast: (a) pH_T range from 4.0 to 12; and (b) pH_T range from 6.5 to 8.5. The arrows in bottom panels (b) indicate changes in carbonate chemistry from surface waters (arrow tail) to $0 \mu\text{mol kg}^{-1}$ dissolved oxygen (arrow head) under present-day and RCP 8.5 scenarios (top and bottom panels, respectively).

West Coast relative to the Gulf of Mexico. Consequently, in colder waters we should observe greater seasonal variability and more rapid response to critical thresholds of acidification and hypercapnia under the higher CO₂ conditions that are expected to occur over the next several decades. These changes should be observable with continuous monitoring of our coastal waters for chemical and biological impacts.

Acknowledgements

This research was supported by the United States National Oceanic and Atmospheric Administration (NOAA), the National Science Foundation (NSF), and the National Aeronautics and Space Administration (NASA). We especially want to thank Libby Jewett and Dwight Gledhill of the NOAA Ocean Acidification Program and Dave Garrison of the National Science Foundation for their support. Nina Bednaršek was supported by the Pacific Marine Environmental Laboratory of NOAA and the NOAA Ocean Acidification Program. Wei-Jun Cai received support from NSF (OCE - 0752110 and 1559279 from the Chemical Oceanography Program), NASA (NNH13ZDA001N and NNX14AM37G) and NOAA Ocean Acidification Program. Robert H. Byrne acknowledges support from the NSF under contract number OCE-1220110. This is PMEL contribution number 4674.

References

- Barton, A., Hales, B., Waldbusser, G., Langdon, C., Feely, R.A., 2012. The Pacific oyster, *Crassostrea gigas*, shows negative correlation to naturally elevated carbon dioxide levels: implications for near-term ocean acidification impacts. *Limnol. Oceanogr.* 57, 698–710. <http://dx.doi.org/10.4319/lo.2012.57.3.0698>.
- Barton, A., Waldbusser, G.G., Feely, R.A., Weisberg, S.B., Newton, J.A., Hales, B., Cudd, S., Eudeline, B., Langdon, C.J., Jefferds, L., King, T., Suhrbier, A., McLaughlin, K., 2015. Impacts of coastal acidification on the Pacific Northwest shellfish industry and adaptation strategies implemented in response. *Oceanography* 28 (2), 146–159. <http://dx.doi.org/10.5670/oceanog.2015.38>.
- Bednaršek, N., Feely, R.A., Reum, J.C.P., Peterson, W., Menkel, J., Alin, S.R., Hales, B., 2014. *Limacina helicina* shell dissolution as an indicator of declining habitat suitability due to ocean acidification in the California Current Ecosystem. *Proc. R. Soc. B* 281, 20140123. <http://dx.doi.org/10.1098/rspb.2014.0123>.
- Bednaršek, N., Harvey, C.J., Kaplan, I.C., Feely, R.A., Možina, J., 2016. Pteropods on the edge: cumulative effects of ocean acidification, warming, and deoxygenation. *Prog. Oceanogr.* 145, 1–24. <http://dx.doi.org/10.1016/j.pocean.2016.04.002>.
- Bednaršek, N., Feely, R.A., Tolimieri, N., Hermann, A.J., Siedlecki, S.A., Waldbusser, G.G., McElhany, P., Alin, S.R., Klinger, T., Moore-Maley, B., Pörtner, H.O., 2017. Exposure history determines pteropod vulnerability to ocean acidification along the US West Coast. *Sci. Rep.* 7, 4526. <http://dx.doi.org/10.1038/s41598-017-03934-z>.
- Booth, A.T., McPhee, E.E., Chua, P., Kingsley, E., Denny, M., Phillips, R., Bograd, S.J., Zeidberg, L.D., Gilly, W.F., 2012. Natural intrusions of hypoxic, low pH water into nearshore marine environments on the California coast. *Cont. Shelf Res.* 45, 108–115.
- Byrne, R.H., Mecking, S., Feely, R.A., Liu, X., 2010. Direct observations of basin-wide acidification of the North Pacific Ocean. *Geophys. Res. Lett.* 37, L02601. <http://dx.doi.org/10.1029/2009GL040999>.
- Cai, W.-J., Hu, X., Huang, W.-J., Murrell, M.C., Lehrter, J.C., Lohrenz, S.E., Chou, W.-C., Zhai, W., Hollibaugh, J.T., Wang, Y., Zhao, P., Guo, X., Gundersen, K., Dai, M., Gong, G.-C., 2011. Acidification of subsurface coastal waters enhanced by eutrophication. *Nat. Geosci.* 4 (11), 766–770. <http://dx.doi.org/10.1038/ngeo1297>.
- Cai, W.-J., Hu, X., Huang, W.-J., Jiang, L.-Q., Wang, Y., Peng, T.-H., Zhang, X., 2010. Alkalinity distribution in the western North Atlantic Ocean margins. *J. Geophys. Res.* 115, C08014. <http://dx.doi.org/10.1029/2009JC005482>.
- Carpenter, J.H., 1965. The Chesapeake Bay Institute technique for the Winkler dissolved oxygen method. *Limnol. Oceanogr.* 10 (1), 141–143. <http://dx.doi.org/10.4319/lo.1965.10.1.0141>.
- Chan, F., Barth, J.A., Lubchenco, J., Kirincich, A., Weeks, H., Peterson, W.T., Menge, B.A., 2008. Emergence of anoxia in the California current large marine ecosystem. *Science* 319 (5865), 920. <http://dx.doi.org/10.1126/science.1149016>.
- Chan, F., Barth, J.A., Blanchette, C.A., Byrne, R.H., Chavez, F., Cheriton, O., Feely, R.A., Friederich, G., Gaylord, B., Gouhier, T., Hacker, S., Hill, T., Hofmann, G., McManus, M.A., Menge, B.A., Nielsen, K.J., Russell, A., Sanford, E., Sevadjian, J., Washburn, L., 2017. Persistent spatial structuring of coastal ocean acidification in the California Current System. *Sci. Rep.* 7, 2526. <http://dx.doi.org/10.1038/s41598-017-02777-y>.
- Comeau, S., Gorsky, G., Alliouane, S., Gattuso, J.P., 2010. Larvae of the pteropod *Cavolinia inflexa* exposed to aragonite undersaturation are viable but shell-less. *Mar. Biol.* 157 (10), 2341–2345.
- Dickson, A.G., 1990a. Standard potential of the reaction: $\text{agcl}(s) + 1/2\text{H}_2(g) = \text{Ag}(s) + \text{HCl}(aq)$, and the standard acidity constant of the ion HSO_4^- in synthetic sea water from 273.15 to 318.15 K. *J. Chem. Thermodyn.* 22, 113–127.
- Dickson, A.G., 1990b. Thermodynamics of the dissociation of boric acid in synthetic seawater from 273.15 to 298.25 K. *Deep-Sea Res.* 37, 755–766.
- Dickson, A.G., Goyet, C., 1994. *Handbook of Methods for the Analysis of the Various Parameters of the Carbon Dioxide System in Sea Water (Version 2)*, ORNL/CDIAC-74. U.S. Department of Energy.
- Dickson, A.G., Sabine, C.L., Christian, J.R., 2007. *Guide to Best Practices for Ocean CO₂ Measurements*. 3. PICES Special Publication, pp. 191.
- Dixon, D.L., Munday, P.L., Jones, G.P., 2010. Ocean acidification disrupts the innate ability of fish to detect predator olfactory cues. *Ecology Lett.* 13, 68–75. <http://dx.doi.org/10.1111/j.1461-0248.2009.01400.x>.
- Doney, S.C., Balch, W.M., Fabry, V.J., Feely, R.A., 2009a. Ocean acidification: a critical emerging problem for the ocean sciences. *Oceanography* 22 (4), 18–27. <http://dx.doi.org/10.5670/oceanog.2009.93>.
- Doney, S.C., Fabry, V.J., Feely, R.A., Kleypas, J.A., 2009b. Ocean acidification: the other CO₂ problem. *Annu. Rev. Mar. Sci.* 1, 169–192.
- Doney, S.C., 2010. The growing human footprint on coastal and open-ocean biogeochemistry. *Science* 328 (5985), 1512–1516. <http://dx.doi.org/10.1126/science.1185198>.
- Egleston, E.S., Sabine, C.L., Morel, F.M.M., 2010. Revelle revisited: buffer factors that quantify the response of ocean chemistry to changes in DIC and alkalinity. *Glob. Biogeochem. Cycles* 24, GB1002. <http://dx.doi.org/10.1029/2008GB003407>.
- Fabry, V.J., Seibel, B.A., Feely, R.A., Orr, J.C., 2008. Impacts of ocean acidification on marine fauna and ecosystem processes. *ICES J. Mar. Sci.* 65, 414–432.
- Feely, R.A., Sabine, C.L., Lee, K., Berelson, W., Kleypas, J., Fabry, V.J., Millero, F.J., 2004. Impact of anthropogenic CO₂ on the CaCO₃ system in the oceans. *Science* 305 (5682), 362–366. <http://dx.doi.org/10.1126/science.1097329>.
- Feely, R.A., Sabine, C.L., Hernandez-Ayon, J.M., Ianson, D., Hales, B., 2008. Evidence for upwelling of corrosive "acidified" water onto the Continental Shelf. *Science* 320 (5882), 1490–1492. <http://dx.doi.org/10.1126/science.1155676>.
- Feely, R.A., Doney, S.C., Cooley, S.R., 2009. Ocean acidification: present conditions and future changes in a high-CO₂ world. *Oceanography* 22 (4), 36–47. <http://dx.doi.org/10.5670/oceanog.2009.95>.
- Feely, R.A., Sabine, C.L., Byrne, R.H., Millero, F.J., Dickson, A.G., Wanninkhof, R., Murata, A., Miller, L.A., Greeley, D., 2012. Decadal changes in the aragonite and calcite saturation state of the Pacific Ocean. *Glob. Biogeochem. Cycles* 26, GB3001. <http://dx.doi.org/10.1029/2011GB004157>.
- Feely, R.A., Alin, S., Carter, B., Bednaršek, N., Hales, B., Chan, F., Hill, T.M., Gaylord, B., Sanford, E., Byrne, R.H., Sabine, C.L., Greeley, D., Juraneck, L., 2016. Chemical and biological impacts of ocean acidification along the west coast of North America. *Estuar. Coast. Shelf Sci.* 183 (A), 260–270. <http://dx.doi.org/10.1016/j.ecss.2016.08.043>.
- Frieder, C.A., Gonzalez, J.P., Bockman, E.E., Navarro, M.O., Levin, L.A., 2014. Can variable pH and low oxygen moderate ocean acidification outcomes for mussel larvae? *Glob. Change Biol.* 20, 754–764.
- Gattuso, J.-P., Hansson, L., 2011. Ocean acidification: background and history. In: Gattuso, J.-P., Hansson, L. (Eds.), *Ocean Acidification*. Oxford Univ. Press, Oxford, pp. 1–20.
- Gattuso, J.-P., Magnan, A., Bille, R., Cheung, W.W.L., Howes, E.L., Joos, F., Allemand, D., Bopp, L., Cooley, S.R., Eakin, C.M., Hoegh-Guldberg, O., Kelly, R.P., Pörtner, H.-O., Rogers, A.D., Baxter, J.M., Laffoley, D., Osborn, D., Rankovic, A., Rochette, J., Sumaila, U.R., Treyer, S., Turley, C., 2015a. Contrasting futures for ocean and society from different anthropogenic CO₂ emission scenarios. *Science* 349 (6243), aac4722. <http://dx.doi.org/10.1126/science.aac4722>.
- Gattuso, J.-P., Epitalon, J.-M., Lavigne, H., 2015b. Seacarb: Seawater Carbonate Chemistry. R package version 3.0.14. (Available at <<https://CRAN.R-project.org/package=seacarb>>).
- Grantham, B.A., Chan, F., Nielsen, K.J., Fox, D.S., Barth, J.A., Lubchenco, J., Menge, B.A., 2004. Upwelling-driven nearshore hypoxia signals ecosystem and oceanographic changes in the northeast Pacific. *Nature* 429 (6993), 749–754. <http://dx.doi.org/10.1038/nature02605>.
- Gruber, N., Hauri, C., Lachkar, Z., Loher, D., Frölicher, T.L., Plattner, G.-K., 2012. Rapid progression of ocean acidification in the California Current System. *Science* 337 (6091), 220–223.
- Guinotte, J.M., Fabry, V.J., 2008. Ocean acidification and its potential effects on marine ecosystems. *Ann. N. Y. Acad. Sci.* 1134, 320–342. <http://dx.doi.org/10.1196/annals.1439.013>.
- Hales, B., Suhrbier, A., Waldbusser, G.G., Feely, R.A., Newton, J., 2017. The carbonate chemistry of the 'fattening line', Willapa Bay, 2011–2014. *Estuar. Coast.* 40 (1), 173–186. <http://dx.doi.org/10.1007/s12237-016-0136-7>.
- Hales, B., Karp-Boss, L., Perlin, A., Wheeler, P., 2006. Oxygen production and carbon sequestration in an upwelling coastal margin. *Glob. Biogeochem. Cycles* 20, GB3001. <http://dx.doi.org/10.1029/2005GB002517>.
- Harris, K.E., DeGrandpre, M.D., Hales, B., 2013. Aragonite saturation state dynamics in a coastal upwelling zone. *Geophys. Res. Lett.* 40, 2720–2725. <http://dx.doi.org/10.1002/grl.50460>.
- Hauri, C., Gruber, N., Vogt, M., Doney, S.C., Feely, R.A., Lachkar, Z., Leinweber, A., McDonnell, A.M.P., Munnich, M., Plattner, G.-K., 2013. Spatiotemporal variability and long-term trends of ocean acidification in the California Current System. *Biogeosciences* 10, 193–216. <http://dx.doi.org/10.5194/bg-10-193-2013>.
- Hettinger, A., Sanford, E., Hill, T.M., Russell, A.D., Sato, K.N., Hoey, J., Forsch, M., Page, H.N., Gaylord, B., 2012. Persistent carry-over effects of planktonic exposure to ocean acidification in the Olympia oyster. *Ecology* 93, 2758–2768.
- Hickey, B.M., 1979. The California current system – hypotheses and facts. *Prog. Oceanogr.* 8, 191–279. [http://dx.doi.org/10.1016/0079-6611\(79\)90002-8](http://dx.doi.org/10.1016/0079-6611(79)90002-8).
- Hofmann, G.E., Todgham, A.E., 2010. Living in the now: physiological mechanisms to tolerate a rapidly changing environment. *Annu. Rev. Physiol.* 72, 127–145.
- Huang, W.-J., Wang, Y., Cai, W.-J., 2012. Assessment of sample storage techniques for total alkalinity and dissolved inorganic carbon in seawater. *Limnol. Ocean. Methods* 10, 711–717. <http://dx.doi.org/10.4319/lom.2012.10.711>.

- Huang, W.-J., Cai, W.-J., Hu, X., Chen, B., Lohrenz, S.E., Chakraborty, S., He, R., Brandes, J., Hopkinson, C.S., 2015. The response of inorganic carbon distribution and dynamics to upwelling favorable winds on the northern Gulf of Mexico during summer. *Cont. Shelf Res.* 111, 211–222. <http://dx.doi.org/10.1016/j.csr.2015.08.020>.
- IPCC, 2013. The Physical Science Basis. Contribution of Working Group I to the Fifth Assessment Report of the Intergovernmental Panel on Climate Change. In: Stocker, T.F., Qin, D., Plattner, G.-K., Tignor, M., Allen, S.K., Boschung, J., Nauels, A., Xia, Y., Bex, V., Midgley, P.M. (Eds.), Cambridge University Press, Cambridge, UK and New York, NY, pp. 1535.
- Johnson, K.M., Sieburth, J.M., Williams, P.J.L., Brändström, L., 1987. Coulometric total carbonate analysis for marine studies: automation and calibration. *Mar. Chem.* 21, 117–133.
- Khan, A.H., Levac, E., Chmura, G.L., 2013. Future sea surface temperatures in large marine ecosystems of the northwest Atlantic. *ICES J. Mar. Sci.* 70, 915–921.
- Kroeker, K.J., Kordas, R.L., Crim, R., Hendriks, I.E., Ramajo, L., Singh, G.S., Duarte, C.M., Gattuso, J.-P., 2013. Impacts of ocean acidification on marine organisms: quantifying sensitivities and interaction with warming. *Glob. Change Biol.* 19, 1884–1896. <http://dx.doi.org/10.1111/gcb.12179>.
- Langdon, C., Atkinson, M.J., 2005. Effect of elevated pCO₂ on photosynthesis and calcification of corals and interactions with seasonal change in temperature/irradiance and nutrient enrichment. *J. Geophys. Res.* 110, C09S07.
- Laurent, A., Fennel, K., Cai, W.-J., Huang, W.-J., Barbero, L., Wanninkhof, R., 2017. Eutrophication-induced acidification of coastal waters in the northern Gulf of Mexico: insights into origin and processes from a coupled physical-biogeochemical model. *Geophys. Res. Lett.* 44, 946–956. <http://dx.doi.org/10.1002/2016GL071881>.
- Lewis, E., Wallace, D.W.R., 1998. Program developed for CO₂ System Calculations. ORNL/CDIAC-105. Carbon Dioxide Information Analysis Center, Oak Ridge National Laboratory, Oak Ridge, Tenn (Available online at). http://cdiac.ornl.gov/ftp/co2sys/CO2SYS_calc_DOS_v1.05/cdiac105.pdf.
- Lischka, S., Buedenbender, J., Boxhammer, T., Riebesell, U., 2011. Impact of ocean acidification and elevated temperatures on early juveniles of the polar shelled pteropod *Limacina helicina*: mortality, shell degradation, and shell growth. *Biogeosciences* 8, 919–932.
- Liu, X., Patsavas, M.C., Byrne, R.H., 2011. Purification and characterization of meta-cresol purple for spectrophotometric seawater pH measurements. *Environ. Sci. Technol.* 45 (11), 4862–4868.
- Lueker, T.J., Dickson, A.G., Keeling, C.D., 2000. Ocean pCO₂ calculated from dissolved inorganic carbon, alkalinity, and equations for K₁ and K₂: validation based on laboratory measurements of CO₂ in gas and seawater at equilibrium. *Mar. Chem.* 70 (1–3), 105–119.
- Mackas, D.L., Galbraith, M.D., 2012. Pteropod time-series from the NE Pacific. *ICES J. Mar. Sci.* 69 (3), 448–459. <http://dx.doi.org/10.1093/icesjms/fsr163>.
- Manno, C., Morata, N., Primicerio, R., 2012. *Limacina retroversa*'s response to combined effects of ocean acidification and sea water freshening. *Estuar. Coast. Shelf Sci.* 113, 163–171.
- McNeil, B.I., Sasse, T.P., 2016. Future ocean hypercapnia driven by anthropogenic amplification of the natural CO₂ cycle. *Nature* 529 (7586), 383–386. <http://dx.doi.org/10.1038/nature16156>.
- Millero, F.J., Zhang, J.Z., Lee, K., Campbell, D.M., 1993. Titration alkalinity of seawater. *Mar. Chem.* 44, 153–165.
- Millero, F.J., 1995. Thermodynamics of the carbon-dioxide system in the oceans. *Geochim. Cosmochim. Acta* 59, 661–677.
- Morris, A.W., Riley, J.P., 1966. The bromide/chlorinity and sulphate/chlorinity ratio in sea water. *Deep Sea Res. Oceanogr. Abstr.* 13, 699–705.
- Mucci, A., 1983. The solubility of calcite and aragonite in seawater at various salinities, temperatures, and one atmosphere total pressure. *Am. J. Sci.* 283, 780–799.
- Nilsson, G.E., Dixon, D.L., Domenici, P., McCormick, M.I., Sorensen, C., Watson, S.-A., Munday, P.L., 2012. Near-future carbon dioxide levels alter fish behaviour by interfering with neurotransmitter function. *Nat. Clim. Change* 2, 201–204. <http://dx.doi.org/10.1038/nclimate1352>.
- O'Donnell, M.J., George, M.N., Carrington, E., 2013. Mussel byssus attachment weakened by ocean acidification. *Nat. Clim. Change* 3, 587–590.
- Ono, T., Watanabe, S., Okuda, K., Fukasawa, M., 1998. Distribution of total carbonate and related properties in the North Pacific along 30°N. *J. Geophys. Res. Oceans* 103, 30873–30883.
- Orr, J.C., Fabry, V.J., Aumont, O., Bopp, L., Doney, S.C., Feely, R.A., Gnanadesikan, A., Gruber, N., Ishida, A., Joos, F., Key, R.M., Lindsay, K., Maier-Reimer, E., Matar, R., Monfray, P., Mouchet, A., Najjar, R.G., Plattner, G.K., Rodgers, K.B., Sabine, C.L., Sarmiento, J.L., Schlitzer, R., Slater, R.D., Totterdell, I.J., Weirig, M.F., Yamanaka, Y., Yool, A., 2005. Anthropogenic ocean acidification over the twenty-first century and its impact on calcifying organisms. *Nature* 437, 681–686.
- Perez, F.F., Fraga, F., 1987. Association constant of fluoride and hydrogen ions in seawater. *Mar. Chem.* 21, 161–168.
- R Core Team, 2016a. R: A Language and Environment for Statistical Computing (Vienna, Austria: R Foundation for Statistical Computing). (Available at <<https://www.R-project.org/>>).
- Redfield, A.C., Ketchum, B.H., Richards, F.A., 1963. The influence of organisms on the chemical composition of seawater. In: Hill, M.N. (Ed.), *The Sea*. Interscience, New York, pp. 26–77.
- Reum, J.C.P., Alin, S.R., Harvey, C.J., Bednaršek, N., Evans, W., Feely, R.A., Hales, B., Lucey, N., Mathis, J.T., McElhany, P., Newton, J., Sabine, C.L., 2016. Interpretation and design of ocean acidification experiments in upwelling systems in the context of carbonate chemistry co-variation with temperature and oxygen. *ICES J. Mar. Sci.* 73, 582–595. <http://dx.doi.org/10.1093/icesjms/fsu231>.
- Riley, J.P., 1965. The occurrence of anomalously high fluoride concentrations in the North Atlantic. *Deep Sea Res. Oceanogr. Abstr.* 12, 219–220.
- Ryckaczewski, R.R., Dunne, J.P., 2010. Enhanced nutrient supply to the California Current Ecosystem with global warming and increased stratification in an earth system model. *Geophys. Res. Lett.* 37 (21), L21606. <http://dx.doi.org/10.1029/2010GL045019>.
- Sabine, C.L., Feely, R.A., Gruber, N., Key, R.M., Lee, K., Bullister, J.L., Wanninkhof, R., Wong, C.S., Wallace, D.W.R., Tilbrook, B., Millero, F.J., Peng, T.-H., Kozyr, A., Ono, T., Rios, A.F., 2004. The oceanic sink for anthropogenic CO₂. *Science* 305 (5682), 367–371. <http://dx.doi.org/10.1126/science.1097403>.
- Sabine, C.L., Tanhua, T., 2010. Estimation of anthropogenic CO₂ inventories in the ocean. *Annu. Rev. Mar. Sci.* 2, 175–198. <http://dx.doi.org/10.1146/annurev-marine-120308-080947>.
- R Core Team, 2016b. R: A Language and Environment for Statistical Computing (Vienna, Austria: R Foundation for Statistical Computing). (Available at <<https://www.R-project.org/>>).
- Siedlecki, S.A., Kaplan, I., Hermann, A.J., Nguyen, T.T., Bond, N.A., Newton, J.A., Williams, G.D., Peterson, W.T., Alin, S.R., Feely, R.A., 2016. Experiments with seasonal forecasts of ocean conditions for the northern region of the California Current upwelling system. *Sci. Rep.* 6, 27203. <http://dx.doi.org/10.1038/srep/27203>.
- Soetaert, K., Petzoldt, T., Meysman, F., 2015. Marelac: Tools for Aquatic Sciences. R Package Version 2.1.5. <<https://CRAN.R-project.org/package=marelac>>.
- Somero, G.N., Beers, J., Chan, F., Hill, T., Klinger, T., Litvin, S., 2016. What changes in the carbonate system, oxygen, and temperature portend for the northeastern Pacific Ocean: a physiological perspective. *Bioscience* 66, 14–26. <http://dx.doi.org/10.1093/biosci/biv162>.
- Sunda, W.G., Cai, W.-J., 2012. Eutrophication induced CO₂-acidification of subsurface coastal waters: interactive effects of temperature, salinity, and atmospheric pCO₂. *Environ. Sci. Technol.* 46 (19), 10651–10659. <http://dx.doi.org/10.1021/es300626f>.
- Thomson, R.E., Krassovski, M.V., 2010. Poleward reach of the California undercurrent extension. *J. Geophys. Res.* 115, C09027. <http://dx.doi.org/10.1029/2010JC006280>.
- Turi, G., Lachkar, Z., Gruber, N., Munnich, M., 2016. Climatic modulation of recent trends in ocean acidification in the California Current System. *Environ. Res. Lett.* 11, 014007. <http://dx.doi.org/10.1088/1748-9326/11/1/014007>.
- UNESCO, 1994. Protocols for the Joint Global Ocean Flux Study (JGOFS) Core Measurements. United Nations Educational, Scientific, and Cultural Organization. http://ijgofs.whoi.edu/Publications/Report_Series/JGOFS_19.pdf.
- Uppström, L.R., 1974. The boron/chlorinity ratio of deep-sea water from the Pacific Ocean. *Deep Sea Res. Oceanogr. Abstr.* 21, 161–162.
- van Vuuren, D., Edmonds, J., Kainuma, M., Riahi, K., Thomson, A., Hibbard, K., Hurtt, G.C., Kram, T., Krey, V., Lamarque, J.-F., Masui, T., Meinshausen, M., Nakicenovic, N., Smith, S.J., Rose, S.K., 2011. The representative concentration pathways: an overview. *Clim. Change* 109, 5–31.
- Waldbusser, G.G., Hales, B., Langdon, C.J., Haley, B.A., Schrader, P., Brunner, E.L., Gray, M.W., Miller, C.A., Gimenez, I., 2015. Saturation state sensitivity of marine bivalve larvae to ocean acidification. *Nat. Clim. Change* 5, 273–280. <http://dx.doi.org/10.1038/nclimate2479>.
- Weisberg, S.B., Bednaršek, N., Feely, R.A., Chan, F., Boehm, A.B., Sutula, M., Ruesink, J.L., Hales, B., Largier, J.L., Newton, J.A., 2016. Water quality criteria for an acidifying ocean: challenges and opportunities. *Ocean Coast. Manag.* 126, 31–41. <http://dx.doi.org/10.1016/j.ocecoaman.2016.03.010>.
- Wood, H.L., Spicer, J.L., Widdicombe, S., 2008. Ocean acidification may increase calcification rates, but at a cost. *Proc. R. Soc. B* 275, 1767–1773.